SSRG International Journal of Electronics and Communication Engineering
ISSN: 2348-8549/ https://doi.org/10.14445/23488549/IJECE-V11I5P122

Volume 11 Issue 5, 235-243, May 2024


*Original Article*

# Design and Implementation of a Miniaturised Microstrip Meander Line Antenna for X-Band Applications

Satyanarayana Raju. K[1], Raju. G. S. N[2], Murali. M[3]

[1,2,3]*Department of Electronics and Communication Engineering, Centurion University, Andhra Pradesh, India.*

[1]*Corresponding Author : kalidindi.Satyanarayanaraju@gmail.com*

Received: 25 March 2024 Revised: 18 April 2024 Accepted: 19 May 2024 Published: 31 May 2024

***Abstract*** *- High-performance antennas are required for radar, satellite, and wireless communication systems. This has led to the necessity for a unique Single Element Microstrip Antenna with a Meander Line for X-band applications. Across the X-band spectrum, conventional designs frequently fall short in terms of performance, efficiency, and compactness. This paper presents a single-element microstrip antenna with a meander line developed, constructed, and simulated for use in X-band applications. The current design considers a FR4 glass epoxy substrate, 1.6 mm thick, with a 4.4 relative permittivity. The intended antenna had a maximum gain of 4.57 dBi, but in real-world use, It was steady at 4.7 dBi of gain between 9.5 GHz to 11 GHz. 11GHz, the designed antenna likewise maintained a return loss of about -21.2748 dB. The new antenna offers better gain, bandwidth, and impedance matching, making it perfect for X-band applications. It does this by utilizing sophisticated techniques such as meander lines and optimizing structure and dimensions.*

***Keywords*** *- Partially Defected Ground (PDGS), Meander Line Antenna (MLA), Antenna, 3D polar plot, Network.*

## 1. Introduction

The need for lightweight, portable antennas that can handle a large frequency spectrum is rising in the current day [1]. Despite their well-known adaptability, microstrip patch antennas frequently have issues with bandwidth and gain limitations [2]. One of the main goals of current research efforts is to overcome these constraints [3]. Designing antennas with appropriate feeding methods and dielectric substrates that function well in particular frequency bands (S, C, X, Ka, and Ku) and offer circular polarization is essential for satellite communications [4]. This design strategy aids receiving base stations in resolving orientation-related problems [5]. Due to its small wavelength, the X-band frequency range is widely used in applications such as military radar, satellite, terrestrial communications, defense tracking, air traffic control, marine vessel traffic management, vehicle speed detection, and weather monitoring [6]. In particular, 8.175 to 8.215 GHz are the frequencies that meteorological satellites use to monitor the weather [8, 9].

A Partly Defective Ground System (PDGS) integrated into the ground plane of a microstrip patch antenna design is suggested as a solution to constraints like restricted bandwidth [10]. Using a microstrip-fed dual-band arrangement with meander lines on the radiating patch, this antenna is intended to function in the 3.2 to 3.8 GHz (Mid-band of Wi-max) and 8 to 12 GHz (X-band) frequencies [11]. Moreover, the use of a meander line antenna design can increase radiation efficiency while reducing antenna size [12]. Meander line antennas are folded antennas that have lower resonance frequencies than single-element antennas of the same length [13, 14]. They are often more radiation efficient than half-wavelength and quarter-wavelength antennas [15]. HFSS was used to simulate an X-band single-element microstrip patch antenna with a meander line [16]. A respectable bandwidth and noteworthy radiation properties, such as enhanced gain, an axial ratio below 3dB, and a tolerable VSWR, were made possible by the Partly Defective Ground System (PDGS) approach [17, 18].

## 2. Antenna Design

This study's miniaturised microstrip patch antenna with a meander line is developed and constructed on an FR4 epoxy substrate with a finite ground plane thickness (h) of 0.16 mm and a relative dielectric permittivity (εr) of 4.4. The antenna is 51.67 mm² (10.825 x 4.775 mm) in size. The substrate edges are placed 0.3 mm from the antenna's top, left, and right edges. Figure 1 shows the specifications of the suggested antenna.

In Figure 1, the FR4 epoxy substrate is indicated by a greenish-yellow color and the patch is indicated by brown color. A microstrip line with width Fw=0.3mm and length Fl=1.6mm is used to feed the antenna from the lower right corner at a distance of Xf=0.003mm with an impedance of 50Ω.

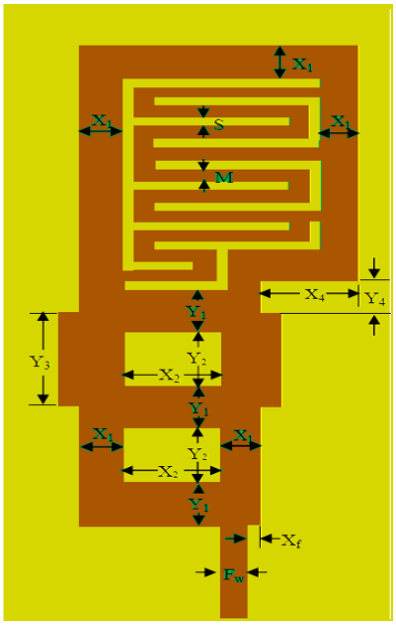


**Microstrip line Feed:**
Feed Distance, $X_f$=0.003mm
Feed width, $F_w$ = 0.300 mm
Feed length, $F_1$ = 1.600 mm
**Power Couplers:**
Width, $X_1$ = 0.600 mm
Width, $X_2$ = 1.350 mm
Length, $Y_1$ = 0.800 mm
Length, $Y_2$ = 1.000 mm
**Distance between coupler and Loop:**
Microstrip loop width,
$X_1$ = 0.600mm
Width, $X_4$ = 1.350 mm
Length, $Y_4$ = 0.550 mm
**Meander Line within loop:**
Meander line width,
M = 0.230 mm
Distance between lines,
S = 0.150 mm
**Stub:** Stub Width, $X_3$ = 0.275 mm
Stub Length, $Y_3$ = 1.700 mm

**Fig. 1 The geometry and dimensions of the proposed antenna**

To stimulate different modes and in order to offer different current paths, two successive power couplers are used with parameters X1=0.6mm and X2=1.35mm in the X-direction, Y1=0.8mm and Y2=1.0mm in the Y-direction. For the matching of impedance, a stub with parameters X3=0.275mm and Y3=1.7mm is added to the second power coupler. A microstrip loop with a width of X1=0.6 mm and parameters X4=1.35 mm and Y4=0.55 mm designate the loop's right lower corner, to which the power couplers are attached. To make the most use of the available area, a meander line inside the loop is positioned with a width of M=0.23 mm and a spacing between lines of S=0.15 mm.

### *2.1. HFSS Design Structure of Single Element Microstrip Patch Antenna Using Meander Technique for X Band*

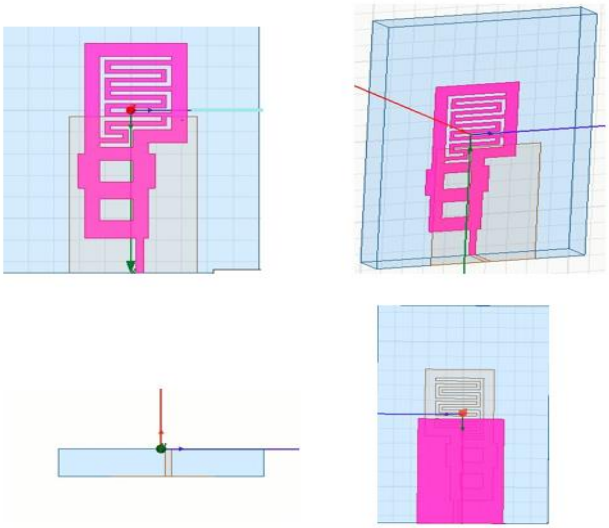

**Fig. 2 Single element micro strip patch antenna for X-Band**

### *2.2. Return Loss*

The percentage of power that is not transferred from the source onto the load is measured by return loss, sometimes referred to as reflection loss. If the load reflects Py and the power received at the load is Px, then the return loss in decibels is

$$R_L(dB) = 10 \log \frac{\text{Px}}{\text{Py}}$$

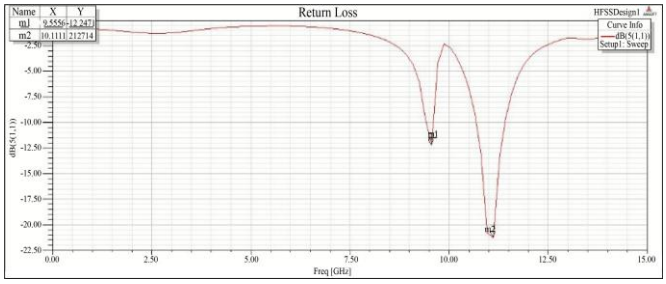


**Fig. 3 Return loss plot of single element micro strip patch antenna for X band**

Figure 3 above illustrates the return loss for the antennae that were built for this study. A returns loss equal to 21.2748 dB is reached at an 11 GHz frequency. The intended result is minimal return power, which is shown by a high return loss in dB.

### *2.3. 3D Polar Plot*

The radiation strength of Antenna gain is the difference between an antenna pointed in a certain direction and an isotropic antenna. The three-dimensional Polar plot is used to represent the gain of the antenna in all three directions, as depicted in Figure 4. The antenna was created and exhibited a gain of 4.57 dB.

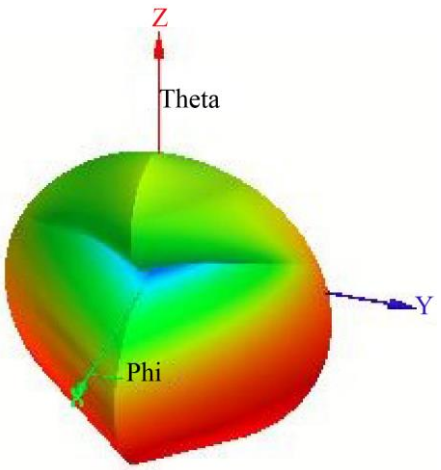


**Fig. 4 3D Polar plot of single element micro strip antenna in X band**

### *2.4. VSWR*

A transmission line's voltage fluctuations are measured using the Voltage Standing Wave Ratio (VSWR), which is the voltage ratio calculated from highest to lowest recorded. It was obtained that the VSWR at 11 GHz is 1.135, whereas the ideal VSWR is between 1 and 2.5 for most wireless applications. Variation of VSWR Single Element Micro Strip Antenna in X band is displayed in Figure 5.

### *2.5. Radiation Pattern*

The pattern of radiation, which represents the radiation intensity, shows how much energy an antenna releases or receives per unit solid angle and is shown in below Figure 6 with a smith chart. The designed antenna in this work shows a good radiation pattern with decent gain value making it suitable for X-Band applications.

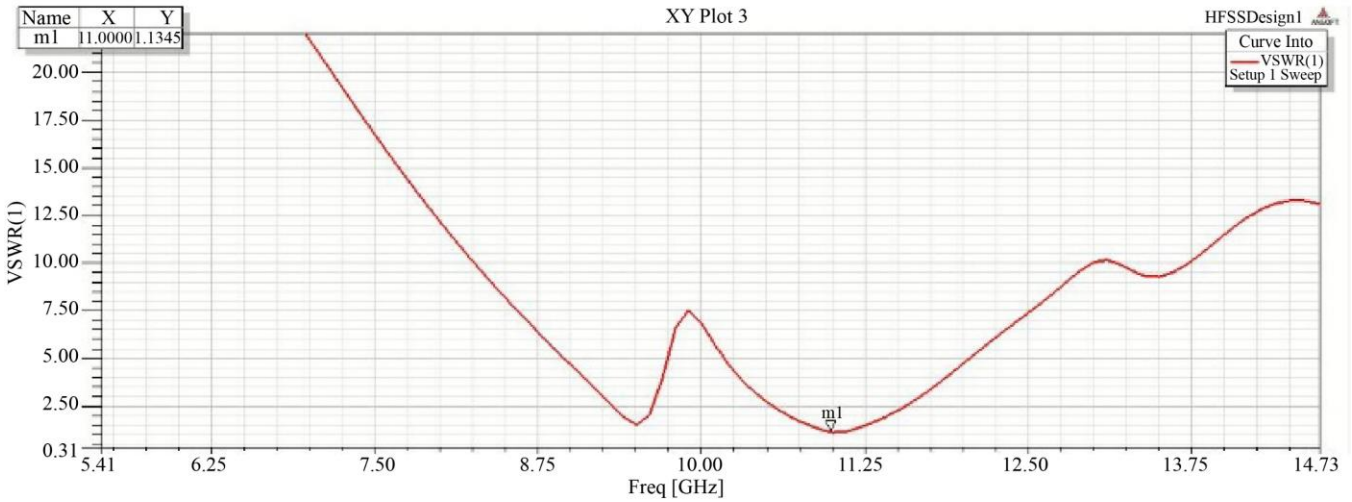


**Fig. 5 Variation of VSWR single element micro strip antenna in X band**

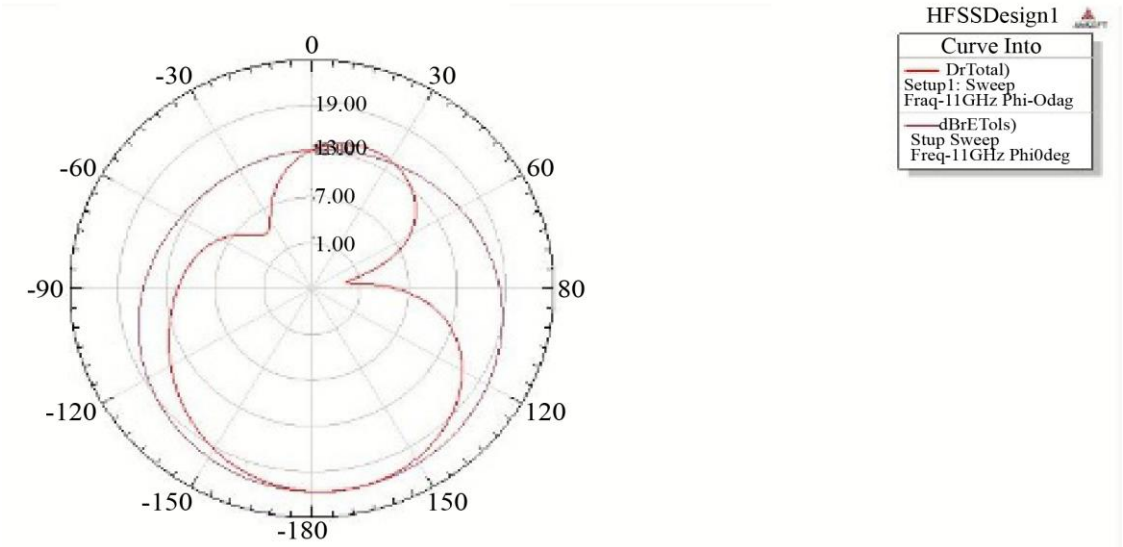


**Fig. 6 Radiation pattern of single element micro strip patch antenna for X band**

The construction of the X-Band Meandering line antenna is depicted in Figure 7.

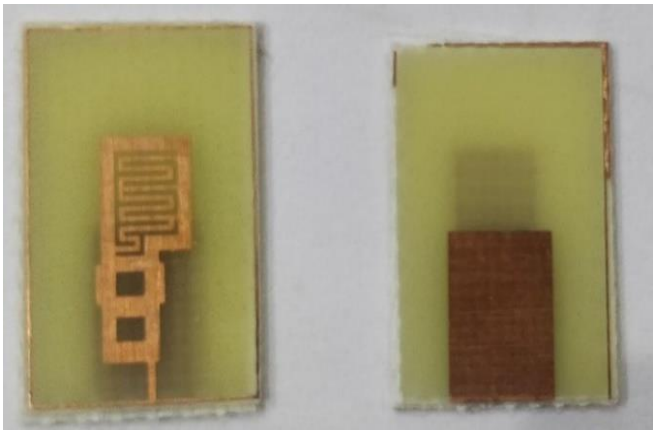

**Fig. 7 X-Band meander line antenna**

**Fig. 8 Fabricated design with connector**

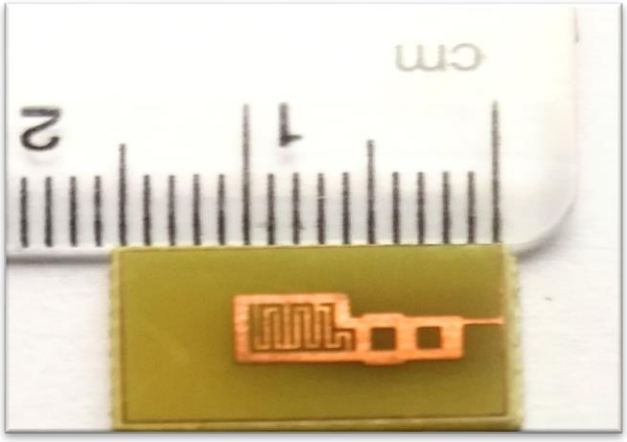

**Fig. 9 Fabricated design antenna of size less than 2 cm**

Parameters like return loss and VSWR were obtained using Network analyzer E5071C. Testing of Fabricated Design by Network Analyzer E5071C is shown in Figure 10.

**Fig. 10 Testing of fabricated design by network analyzer E5071C**

**Fig. 11 Testing of fabricated design by network analyzer E5071C**

The following Figure 12 depicts the Return loss obtained using Network analyzer E5071C.

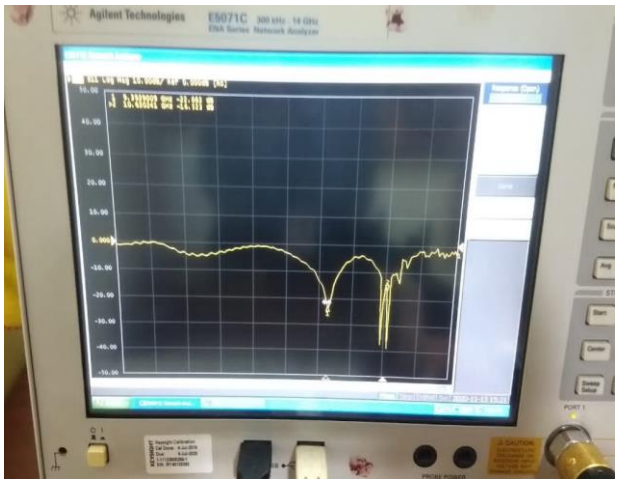


**Fig. 12 Return loss obtained by network analyzer E5071C**

The following Figure 13 depicts the VSWR obtained using Network analyzer E5071C.

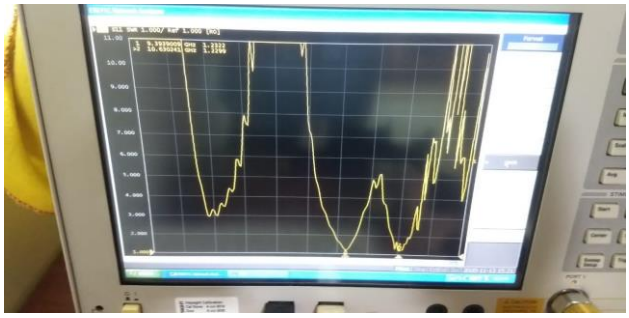

**Fig. 13 VSWR obtained by network analyzer E5071C**

The following Figure 14 depicts the Radiation pattern obtained using Network analyzer E5071C.

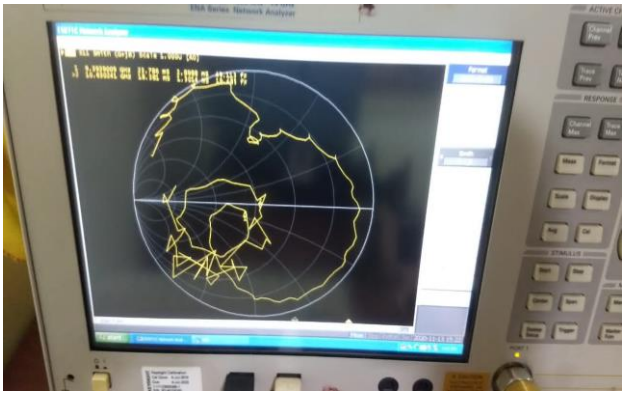

**Fig. 14 Radiation pattern obtained by network analyzer E5071C**

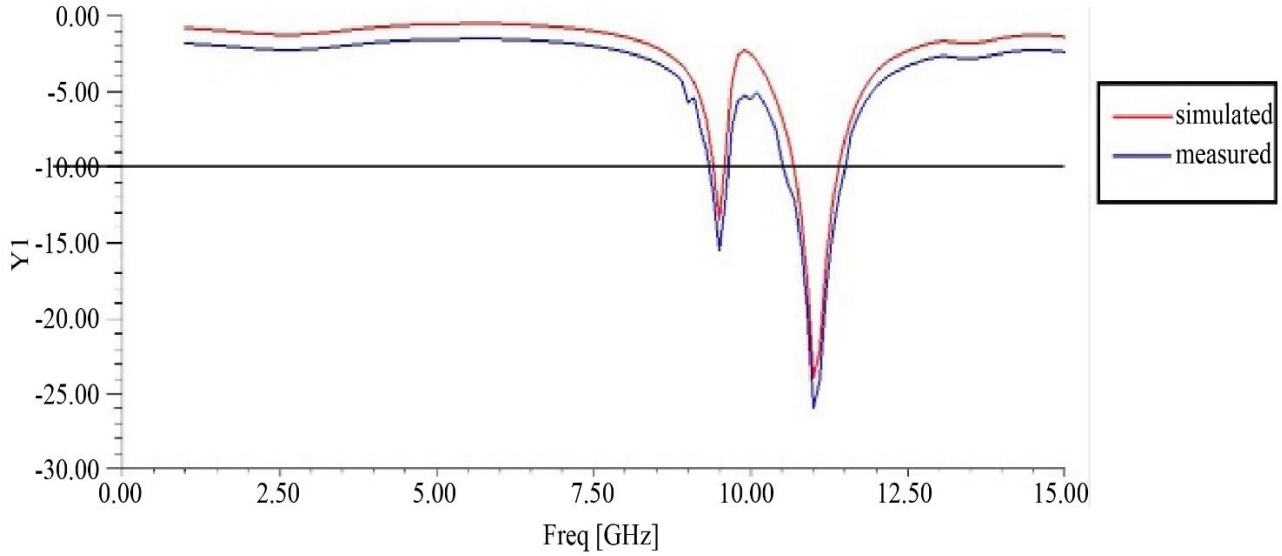


**Fig. 15 Comparison of the measured and simulated return losses**

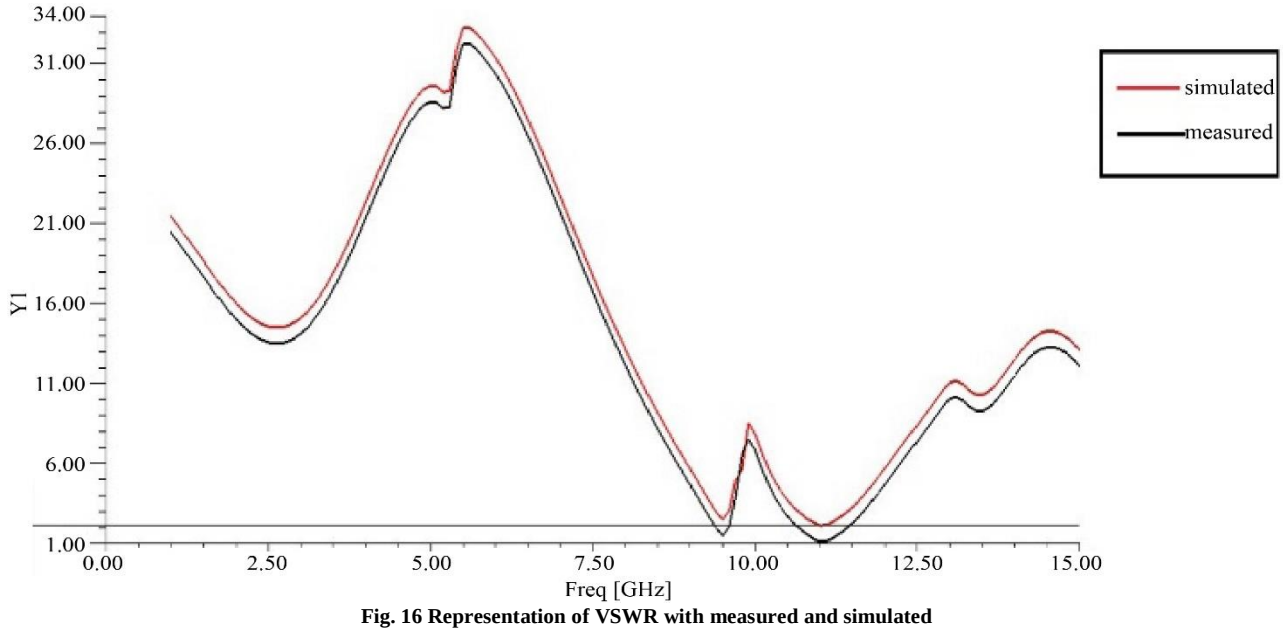


**Fig. 16 Representation of VSWR with measured and simulated**

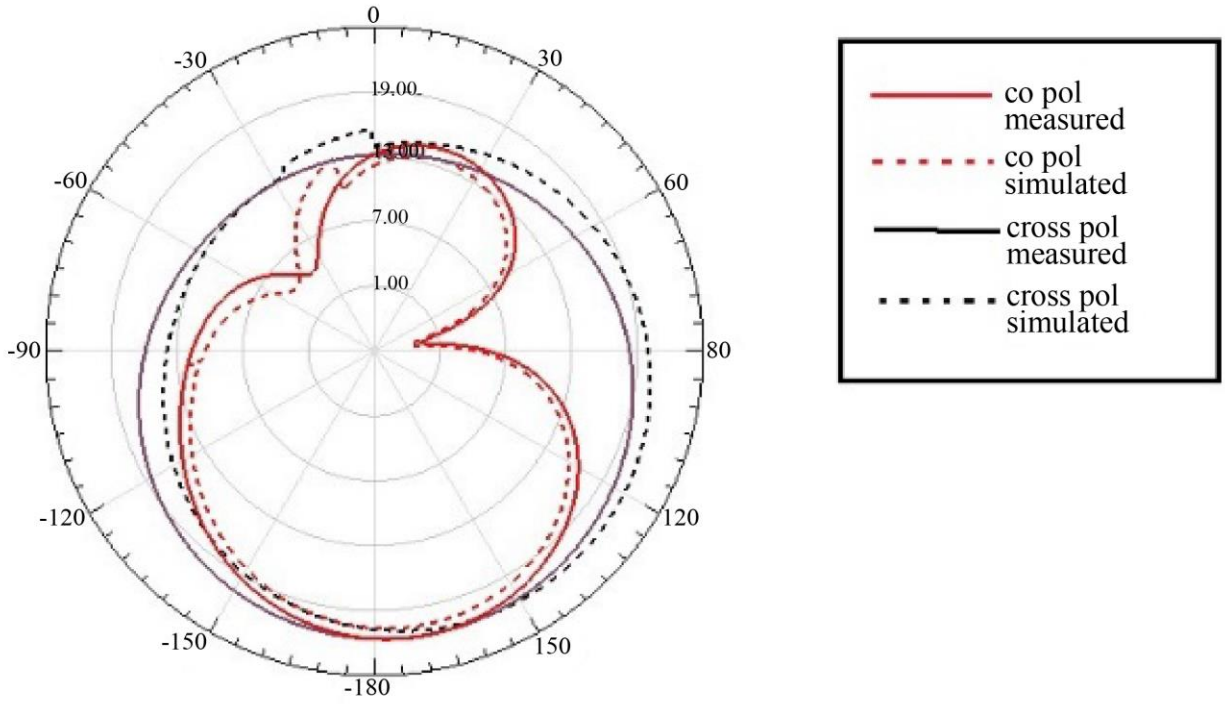


**Fig. 17 Representation of radiation pattern with measured and simulated**

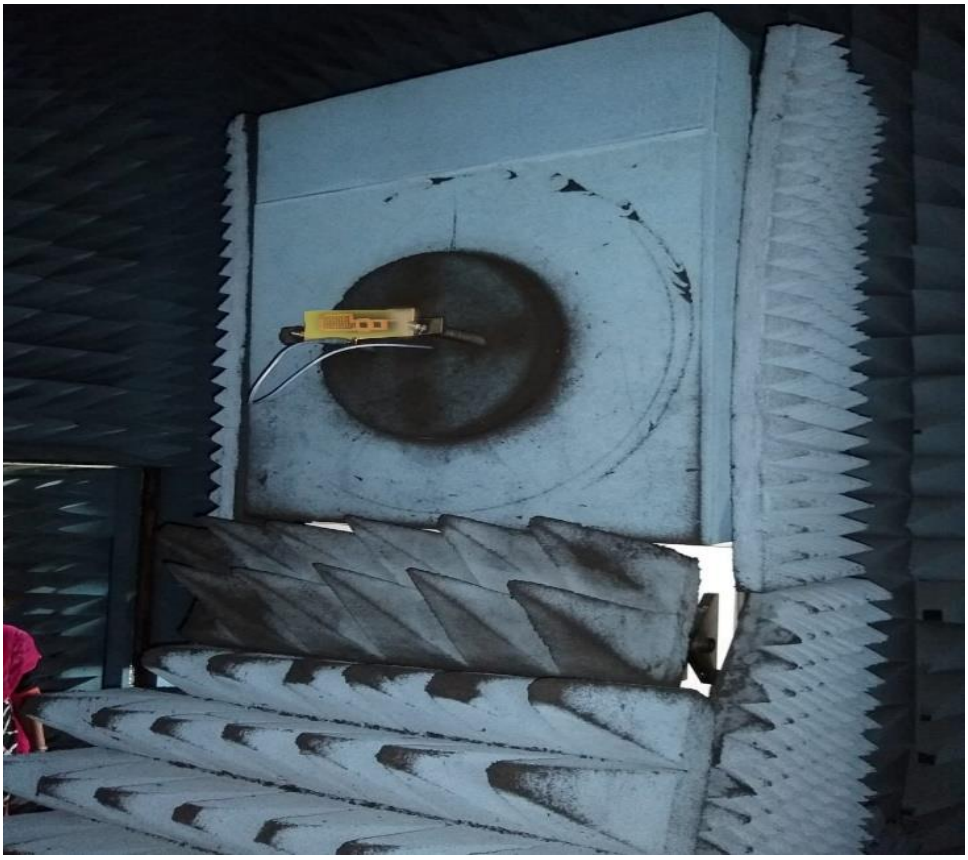

**Fig. 18 Testing of fabricated design in anechoic chamber**

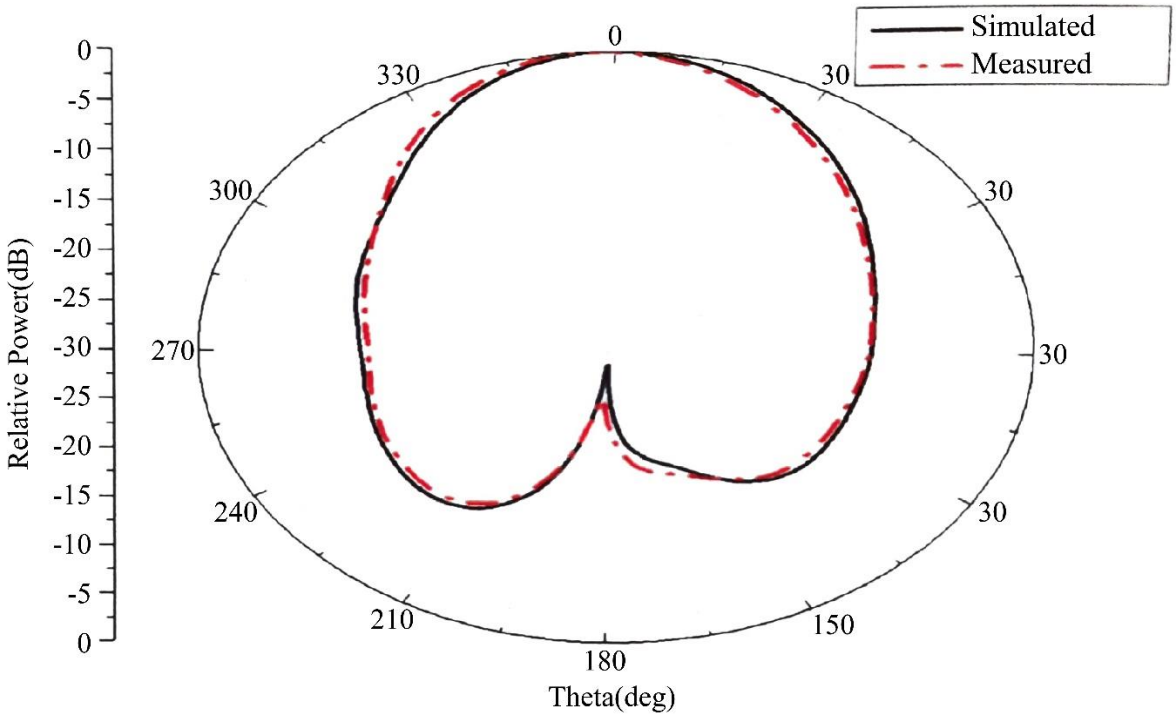


**Fig. 19 Radiation pattern of fabricated design**

**Table 1. Comparison of results between HFSS results and network analyzer output**

| Parameters | Simulated Values | Measured Values |
|---|---|---|
| Resonant Frequency (GHz) | 11 | 10.63 |
| Return Loss (dB) | -21.2748 | -23.992 |
| VSWR | 1.135 | 1.2299 |
| Gain (dBi) | 4.5747 | 4.7 |

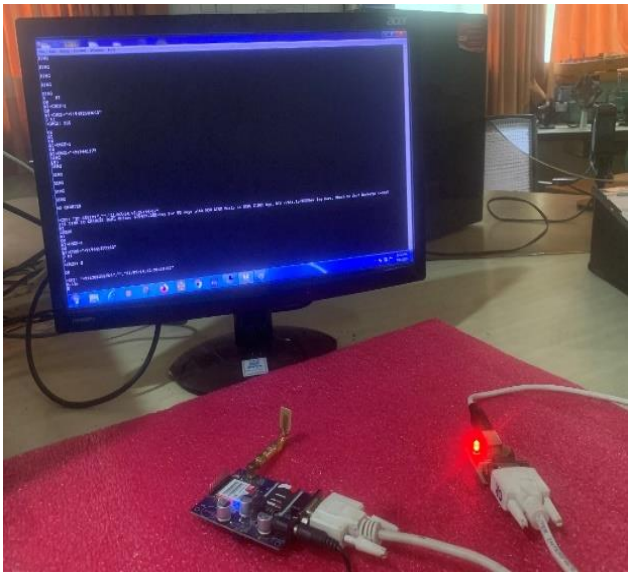

**Fig. 20 Testing of fabricated design in Real-time mobile application through IOT**

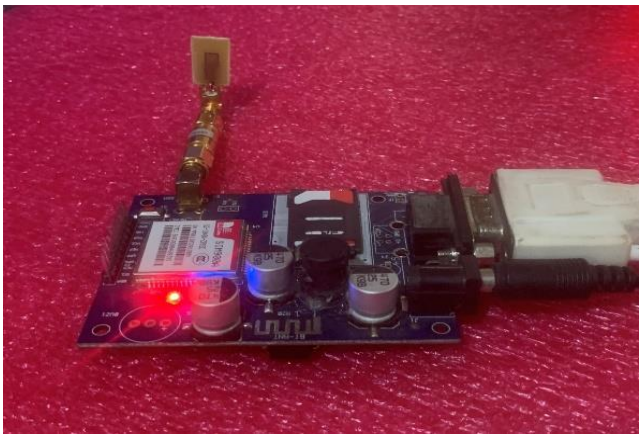

**Fig. 21 Integration of fabricated design with IOT-Sim900 module**

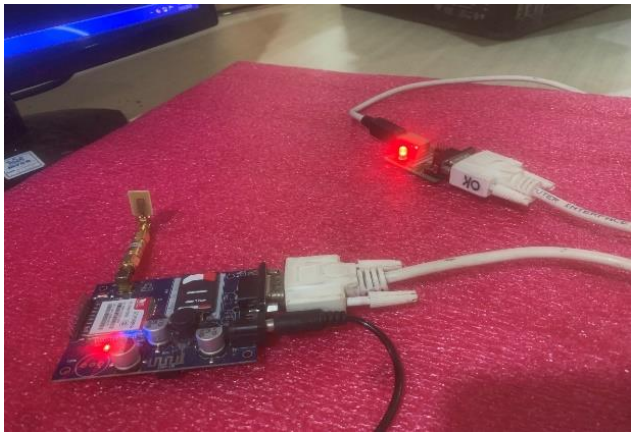

**Fig. 22 Transmission of messages by fabricated design through GSM module**

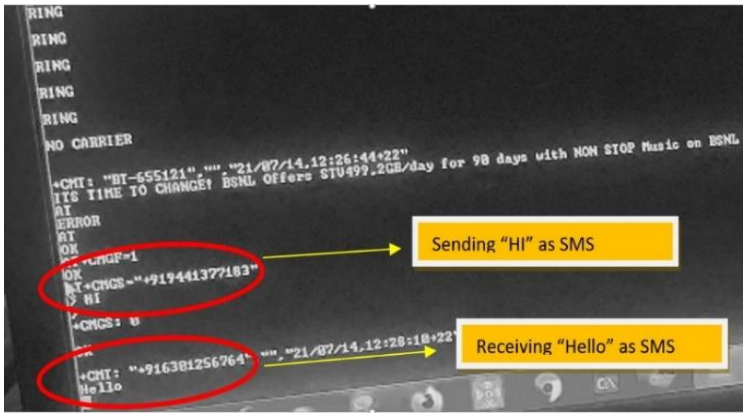


**(a)**

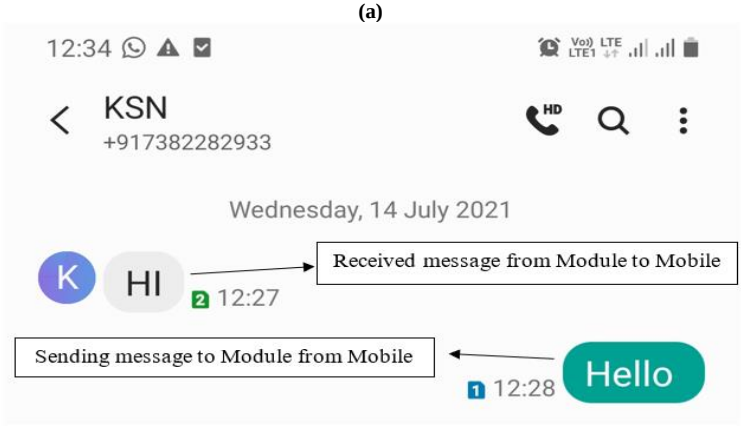


**(b)**

**Fig. 23(a) Depicting sending and receiving of SMS in the console, and (b) Depicting sending and receiving of SMS in mobile.**

## 3. Conclusion

The single element microstrip antenna with a meander Line in X-band applications with a probe feed strategy was designed and implemented. The FR4 glass epoxy substrate, with a 1.6 mm thickness and 4.4 relative permittivity, is taken into consideration. During evaluation with network analyzer E507, with a maximum gain of 4.57 dBi, in the resonance frequency range of 9.5 GHz - 11 GHz. In simulation and 4.7 dBi in a real-world scenario. At 11GHz, the designed antenna maintained a return loss of around 21.2748 dB. Also, tested the fabricated design in real-time mobile applications through IOT using SIM900A module which successfully transmitted and received text messages to and from mobile.

## Acknowledgments

The author would like to express his heartfelt gratitude to the supervisor for his guidance and unwavering support during this research for his guidance and support.

## References

[1] Derneryd, "A Theoretical Investigation of the Rectangular Microstrip Antenna Element," *IEEE Transactions on Antennas and Propagation*, vol. 26, no. 4, pp. 532-535, 1978. [CrossRef] [Google Scholar] [Publisher Link]

[2] J. Rashed, and C.T. Tai, "A New Class of Resonant Antennas," *IEEE Transactions on Antennas and Propagation*, vol. 39, no. 9, pp. 1428-1430, 1991. [CrossRef] [Google Scholar] [Publisher Link]

[3] Shan-Cheng Pan, and Kin-Lu Wong, "Dual-Frequency Triangular Micro Strip Antenna with a Shorting Pin," *IEEE Transactions on Antennas and Propagation*, vol. 45, no. 12, pp. 1889-1891, 1997. [CrossRef] [Google Scholar] [Publisher Link]

[4] T.J. Warnagiris, and T.J. Minardo, "Performance of a Meandered Line as an Electrically Small Transmitting Antenna," *IEEE Transaction on Antennas and Propagation*, vol. 46, no. 12, pp. 1797-1801, 1998. [CrossRef] [Google Scholar] [Publisher Link]

[5] A. Hoorfar, and A. Perrotta, "An Experimental Study of Microstrip Antennas on Very High Permittivity Ceramic Substrates and Very Small Ground Planes," *IEEE Transactions on Antennas and Propagation*, vol. 49, no. 5, pp. 838-840, 2001. [CrossRef] [Google Scholar] [Publisher Link]

[6] S.R. Best, and J.D. Morrow, "Limitations of Inductive Circuit Model Representations of Meander Line Antennas," *IEEE Antennas and Propagation Society International Symposium. Digest. Held in conjunction with: USNC/CNC/URSI North American Radio Sci. Meeting (Cat. No.03CH37450)*, Columbus, OH, USA, vol. 1, pp. 852-855, 2003. [CrossRef] [Google Scholar] [Publisher Link]

[7] H. Mosallaei, and K. Sarabandi, "Antenna Miniaturization and Bandwidth Enhancement Using a Reactive Impedance Substrate," *IEEE Transactions on Antennas and Propagation*, vol. 52, no. 9, pp. 2403-2414, 2004. [CrossRef] [Google Scholar] [Publisher Link]

[8] C.M. Allen et al., "Dual Tapered Meander Slot Antenna for Radar Applications," *IEEE Transactions on Antennas and Propagation*, vol. 53, no. 7, pp. 2324-2328, 2005. [CrossRef] [Google Scholar] [Publisher Link]

[9] O.P.N. Calla et al., "Empirical Relation for Designing the Meander Line Antenna," *2008 International Conference on Recent Advances in Microwave Theory and Applications*, Jaipur, India, pp. 695-697, 2008. [CrossRef] [Google Scholar] [Publisher Link]

[10] Zhonghao Hu, Peter H. Cole, and Linxi Zhang, "A Method for Calculating the Resonant Frequency of Meander-Line Dipole Antenna," *2009 4th IEEE Conference on Industrial Electronics and Applications*, Xi'an, China, pp. 1783-1786, 2009. [CrossRef] [Google Scholar] [Publisher Link]

[11] D. Misman et al., "Design of Dual Beam Meandear Line Antenna," *Proceedings of the 5th European Conference on Antennas and Propagation*, Rome, Italy, pp. 576-578, 2011. [Google Scholar] [Publisher Link]

[12] George Casu, Cătălin Moraru, and Andrei Kovacs, "Design and Implementation of Microstrip Patch Antenna Array," *2014 10th International Conference on Communications*, Bucharest, Romania, pp. 1-4, 2014. [CrossRef] [Google Scholar] [Publisher Link]

[13] Ravi Prakash Dwivedi, Usha Kiran Kommuri, and Veeramani, "Design and Simulation of Wideband Patch Antenna for Wireless Application," *2015 2nd International Conference on Signal Processing and Integrated Networks*, Noida, India, pp. 15-18, 2015. [CrossRef] [Google Scholar] [Publisher Link]

[14] M. Ahmed Hamdi Abo Absa, Mohamed Ouda, and Ammar Abu Hudrouss, "Analysis and Design of E-shape Meander Line Antenna for LTE Mobile Communications," *Journal of Engineering Research and Technology*, vol. 2, no. 1, pp. 75-79, 2015. [Google Scholar]

[15] Vivek Singh, Brijesh Mishra, and Rajeev Singh, "A Compact and wide Band Microstrip Patch Antenna for X-band Applications," *2015 Second International Conference on Advances in Computing and Communication Engineering*, Dehradun, India, pp. 296-300, 2015. [CrossRef] [Google Scholar] [Publisher Link]

[16] Parag Jain et al., "Microstrip Patch antenna for 5G Applications," *2023 International Conference on Advances in Electronics, Communication, Computing and Intelligent Information Systems*, Bangalore, India, pp. 349-353, 2023. [CrossRef] [Google Scholar] [Publisher Link]

[17] Muhammad Saqib Rabbani, and Hooshang Ghafouri-Shiraz, "Liquid Crystalline Polymer Substrate-Based THz Microstrip Antenna Arrays for Medical Applications," *IEEE Antennas and Wireless Propagation Letters*, vol. 16, pp. 1533-1536, 2017. [CrossRef] [Google Scholar] [Publisher Link]

[18] Muhammad Irfan Khattak et al., "Elliptical Slot Circular Patch Antenna Array with Dual Band Behaviour for Future 5G Mobile Communication Networks," *Progress in Electromagnetics Research C*, vol. 89, pp. 133-147, 2019. [CrossRef] [Google Scholar] [Publisher Link]